Eur. Phys. J. D **10**, 147–151 (2000)

THE EUROPEAN PHYSICAL JOURNAL D

EDP Sciences

Electron excitation coefficients for 2p and 3p levels of Xe

G.N. Malović[1], A.I. Strinić[1], Z.Lj. Petrović[1,a], J.V. Božin[1,2], and S.S. Manola[1]

[1] Institute of Physics, Pregrevica 118, P.O.B. 68, 11080 Zemun Belgrade, Yugoslavia
[2] Faculty of Physics, University of Belgrade, P.O.B. 550, 11001 Belgrade, Yugoslavia

Received 17 March 1999 and Received in final form 9 August 1999

Abstract. Electron excitation rate coefficients for $2p$ ($2p_1$, $2p_2$, $2p_3$, $2p_4$, $2p_5$, $2p_6$) and $3p$ ($3p_5$, $3p_6$, $3p_7$, $3p_8$, $3p_{10}$) (in Paschen notation) levels of xenon atom have been measured by using electron drift tube technique. The absolute excitation coefficients were obtained from the optical signal at the anode in Townsend xenon discharges, after correction for detector quantum efficiency. The ionization coefficients were determined from the spatial emission profile. The measurement were made for the electric field to xenon atom number density ratios (E/N) from 90×10^{-21} Vm^2 to 10×10^{-18} Vm^2. The data were obtained between moderate E/N values where electrons are in equilibrium and very high E/N values where electrons may not be in equilibrium with the local field. It was found that at the highest values of E/N heavy particles do not contribute to the excitation under the present conditions. The absolute excitation coefficients for the studied levels of xenon are to our knowledge the only experimental data available in the literature.

PACS. 52.20.Fs Electron collisions – 52.25.Rv Emission, absorption, and scattering of visible and infrared radiation – 52.80.Dy Low-field and Townsend discharges

1 Introduction

Xenon plasmas are widely used for fundamental plasma spectroscopy studies and in numerous applications. Understanding the energy relaxation mechanisms for the excited levels of Xe is of practical importance for modeling kinetic processes in discharge devices, such as excimer lasers (Xe-halide and Xe-metal systems) [1] and xenon atom lasers [2], in microwave after glows [3] and in actinometry [4]. Xenon is also often used in a number of applications including: high energy particles detectors [5,6], plasma thrusters [7] and sputtering for thin film production [8–10].

Recently studies of excitation kinetics in xenon have received a lot of attention due to its application is in plasma displays [11,12]. A mixture of neon and xenon is most frequently used in such devices and the role of neon is to decrease the operating voltage, while xenon in an active source of UV photons.

In this paper we present the first measurements of the absolute excitation coefficients for the $2p$ ($2p_1$, $2p_2$, $2p_3$, $2p_4$, $2p_5$, $2p_6$) and higher states $3p$ ($3p_5$, $3p_6$, $3p_7$, $3p_8$, $3p_{10}$) of xenon by using a drift-tube technique. We will use Paschen notation for simplicity.

We apply a similar technique that has been used in our previous measurements in argon [13], hydrogen [14], nitrogen [15] and neon [16]. The experimental set-up and procedure are described in Section 2. Experimental results are given in Section 3.

[a] e-mail: zoran@petrovic.phy.bg.ac.yu
or e-mail: nzpetr@eunet.yu

2 Experimental set-up and procedure

The experimental apparatus and technique have been described in detail in previous publications from this laboratory [14]. The drift tube is the same as used for the measurement of the excitation coefficients of the $2p$ levels of neon [16] and argon [13]. The tube has two parallel electrodes of 7.9 cm in diameter separated by 1.7 cm. The cathode was made of stainless steel and the anode of vacuum-grade sintered graphite while a closely fitting quartz tube is used to prevent the long path breakdown [17].

Typical operating DC current was 2 μA and was measured by a calibrated electrometer. The lower limit of E/N in the experiment was determined by the onset of oscillations [18].

The drift tube was evacuated down to 10^{-7} torr by a turbomolecular pump before each run. Research-grade xenon gas of 99.999% nominal purity was used without further purification. The gas pressure was from 0.09 torr to 6 torr and it was measured by a capacitance manometer.

The light emitted from the xenon discharge was detected through the quartz window of the vacuum chamber by using a photon-counting chain. The system was calibrated for the wavelength region 330–830 nm by a standard tungsten ribbon lamp as explained in our previous publications [13,14,16]. The selection of lines was done by a Jobin Yvon M25 monochromator with a spectral resolution of 0.7 nm, equipped with a 610 grooves/mm grating blazed at 500 nm and a cooled Hamamatsu R758 photomultiplier tube. Spatial resolution of 0.2 mm was

Table 1. Wavelengths, Einstein coefficients and quenching coefficients for xenon levels used in the present study.

transition	λ (nm)	A_{ij} (10^6 s^{-1})	A_j (10^6 s^{-1})	k_q (10^{-17} m^{-3}s^{-1})
$2p_1$–$1s_2$	458.3	3.02	35.21	26.4
$2p_1$–$1s_4$	788.7	21.8		
$2p_2$–$1s_3$	764.2	14.5	36.76	48.0
$2p_2$–$1s_5$	450.1	0.359		
$2p_3$–$1s_4$	473.5	1.07	36.10	26.0
$2p_4$–$1s_5$	469.1	0.387	26.73	
$2p_5$–$1s_4$	828.0	44.5	44.64	0.58
$2p_6$–$1s_5$	823.2	24.9	35.59	9.22
$3p_5$–$1s_4$	480.7	5.12	16.64	42.0
$3p_6$–$1s_5$	462.4	4.98	13.33	28.4
$3p_7$–$1s_3$	796.7	5.91	16.84	33.0
$3p_8$–$1s_5$	467.1	3.69	9.52	28.0
$3p_{10}$–$1s_4$	502.9	0.023	8.197	28.0

achieved by a collimator while the whole detection system was placed on a platform and moved by a stepper motor.

The experimental procedure for determining the excitation coefficients has been discussed in detail previously [13]. The spatial profiles of xenon lines show an exponential increase of the intensity as we scan from the cathode to the anode which allowed us to determine the ionization coefficients at different E/N. Deconvolution of the profile also gives the anode position and the anode signal S_a [13]. Electron excitation coefficients of the level m are related to the emission signal S_a by [13]:

$$\frac{\varepsilon_m}{N} = \frac{S_a(z)e}{K_{mn} j_e(z) N} \left(1 + \frac{N}{N_{0m}}\right)$$

where $j_e(z)$ is the current density at the position z and z is the distance from the cathode. The quenching density N_0 is given by $N_0 = A_m/k_q$, where k_q is the rate coefficient for collisional quenching of the state m. The constant K_{mn} is given by [13]:

$$K_{mn} = (\Omega/4\pi) V \frac{A_{mn}}{A_m} \int F(\lambda) Q(\lambda) T(\lambda) \mathrm{d}\lambda.$$

Here Ω is the effective solid angle subtended by the detector at the axis of the drift tube, and V is the discharge volume from which the detected radiation was emitted. Factor F is the fractional transmission of the quartz tube, Q is the quantum efficiency of the monochromator, photomultiplier and the counting chain, T is the fractional transmission of the monochromator. A_m/A_{mn} is the ratio of the intensity of the total radiation emitted from the state m to that emitted *via* transition mn.

In Table 1 we show wavelengths, Einstein coefficients and quenching coefficients for all measured transitions in xenon. The data for the transition probabilities were taken from Aymar and Coulombe [19]. The quenching data for different xenon levels were taken from references [20,21].

3 Results and discussion

3.1 Spatial scans and ionization coefficients

The emission from the $2p$ and $3p$ states of xenon atoms to $1s$ states are mainly in the 450–3000 nm spectral region. These levels radiate in transition to the Xe $(6s(3/2)_{1,2})$ states in the 450–490 nm range and to the Xe $(6s'(1/2)_{0,1})$ states in the 760–930 nm range. Radiative transitions to the $5d$ and $7s$ manifolds have wavelengths longer than 1100 nm. The detection system used in this experiment is limited to wavelengths lower than 830 nm. For this reason, it was not possible to record the spectral lines which correspond to the $2p_7$...$2p_{10}$–$1s$ transitions. Having recorded the spectra of selected lines with a higher resolution, for both high and low E/N, we eliminated lines which overlap with nearby atomic or ionic lines. For $3p_9$ level, we could not find, under the limitations of our present setup, any lines which were free from the influence of the nearby lines so it was not included in our measurements.

Spatial profiles of emission of the atomic line (normalized to the discharge current) originating from $2p_1$ are shown in Figure 1 at three different E/N. The positions of the electrodes are shown by vertical dashed lines.

Spatial distribution of emission is quite similar for all other lines from $2p$ and $3p$ levels. However, in case of xenon, unlike lighter rare gases, there is no significant growth of emission towards the cathode [13,16,17]. This means that under the present conditions the excitation by heavy particles (atoms and ions) is small [22]. This, however does not necessarily mean that the cross-sections for heavy particle excitation are smaller but that conditions favouring heavy particle excitation have not been reached in xenon discharge at these E/N and interelectrode spacing.

In Figure 2 we show the ionization coefficients for xenon as a function of E/N. Our results, shown as crosses, were obtained from exponential slopes of spatial scans of emission intensities at different E/N and for different $2p$

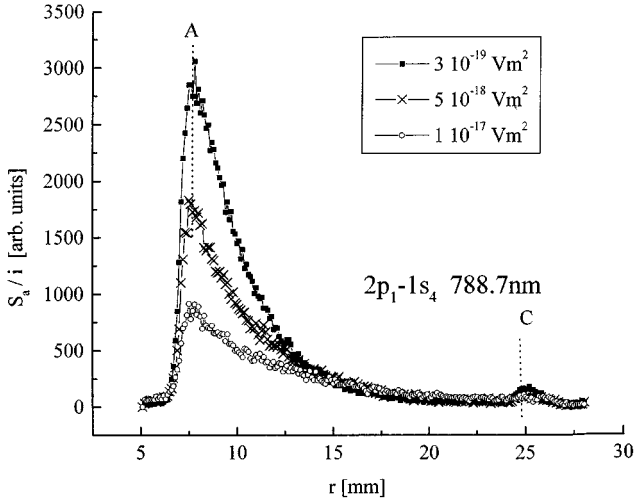

Fig. 1. Spatial distribution of normalized emission of the 788.7 nm line, ($2p_1$–$1s_4$ transition) at three different E/N. A: anode; C: cathode.

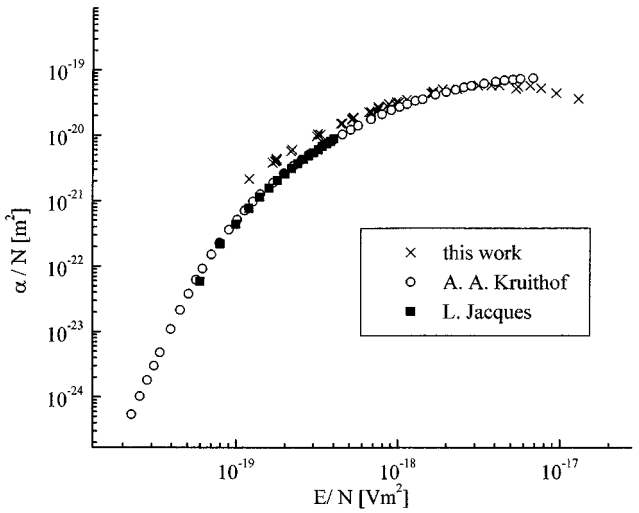

Fig. 2. Ionization coefficients obtained from the slopes of emission profiles (crosses). We also include the data of Kruithof [23] and Jacques *et al.* [24].

and $3p$ transitions. Also included in the figure are the results from Kruithof [23] and Jacques *et al.* [24].

Little work has been done on ionization coefficients in xenon since the early experiments of Kruithof [23] whose results of which are still widely used as the main source of data. Recent measurements [24,25] were performed for relatively narrow ranges of reduced electric field (50×10^{-21} Vm^2 $< E/N < 400 \times 10^{-21}$ Vm^2). Our results for higher values of reduced electric fields have a maximum ($E/N \approx 5 \times 10^{-18}$ Vm^2), after which the coefficient decreases, which is not the case with the results from Kruithof. This is similar to the case of argon [13]. Ionization coefficients depend strongly on excitation cross-sections and can be used as a test of consistency for the whole set of collision cross-sections.

The uncertainty of our results is large, of the order of 5–10%. Nevertheless these results may be useful as a check of consistency of our data with other, more accurate, sources and are sufficiently good fit some applications. The accuracy is poorer at low E/N due to smaller signals which explains a disagreement with other sources of data below 200×10^{-21} Vm^2. Nevertheless the level of agreement with outher sources serves as a good check of consistency of our data and conditions of measurement.

3.2 Excitation coefficients

The spatial distribution of emission at the anode is normalized to give the excitation coefficient. In Figure 3 ($2p_1$ and $2p_4$ in Fig. 3a; $2p_3$, $2p_5$ and $2p_6$ in Fig. 3b and $2p_2$ in Fig. 3c). We show the results for the spatial excitation coefficients for the $2p$ levels of xenon. As E/N increases the number of electrons which have sufficient energy to excite this state increases rapidly. With further increase of E/N, the average electron energy approaches the energy of the maximum of the cross-section and the value of excitation coefficients becomes saturated. For even higher values of E/N, a decrease of the excitation coefficients is observable, which is in agreement with the shape of the cross-sections. The maximum values of excitation coefficients for $2p$ levels are in the range 2–3×10^{-18} Vm^2.

The xenon $2p_1$ level (Fig. 3a) is isolated from other $6p'$ states ($2p_2$ is 581 cm^{-1} lower), but it is between two $6d$ levels ($4d_2$ is 172 cm^{-1} higher and $4d'_1$ is 325 cm^{-1} lower) so it can be collisionally coupled with these levels and it still has a large quenching rate.

The data for the $2p_2$ level as a function of E/N are given in Figure 3c, based on measurements for two transitions $2p_2$–$1s_3$ (764.2 nm) and $2p_2$–$1s_5$ (450.1 nm). The agreement between the two sets of data is good, within the uncertainty of the data particularly if we take into account a considerable difference in wavelengths between the two transitions and a very large difference in transition probabilities (see Tab. 1).

In Figure 4 ($3p_6$ and $3p_8$ in Fig. 4a and $3p_5$, $3p_7$ and $3p_{10}$ in Fig. 4b) we show the excitation coefficients for $3p$ levels of xenon as a function E/N. Cascading from the upper ns and nd levels can repopulate the $3p$ levels but this is not as important as in the case of $2p$ levels. For the $3p$ levels collisions can result in intramultiplet relaxation to lower $3p$ levels or in intermultiplet transfer to the $1s$ and $1s'$ levels. Consequently the quenching is also quite large [26] and as important in the kinetics of these levels as it is in the kinetics of $2p$ levels.

In the present conditions self-quenching has a large effect on the final results for the excitation coefficients. The quenching coefficients for xenon from different references are in good agreement [20,21], so we have confidence in them but if a better set of data becomes available our results can be easily reanalyzed. The uncertainty of our data ranges from ±10% to ±20% depending on the statistics of different lines especially at the low end of E/N.

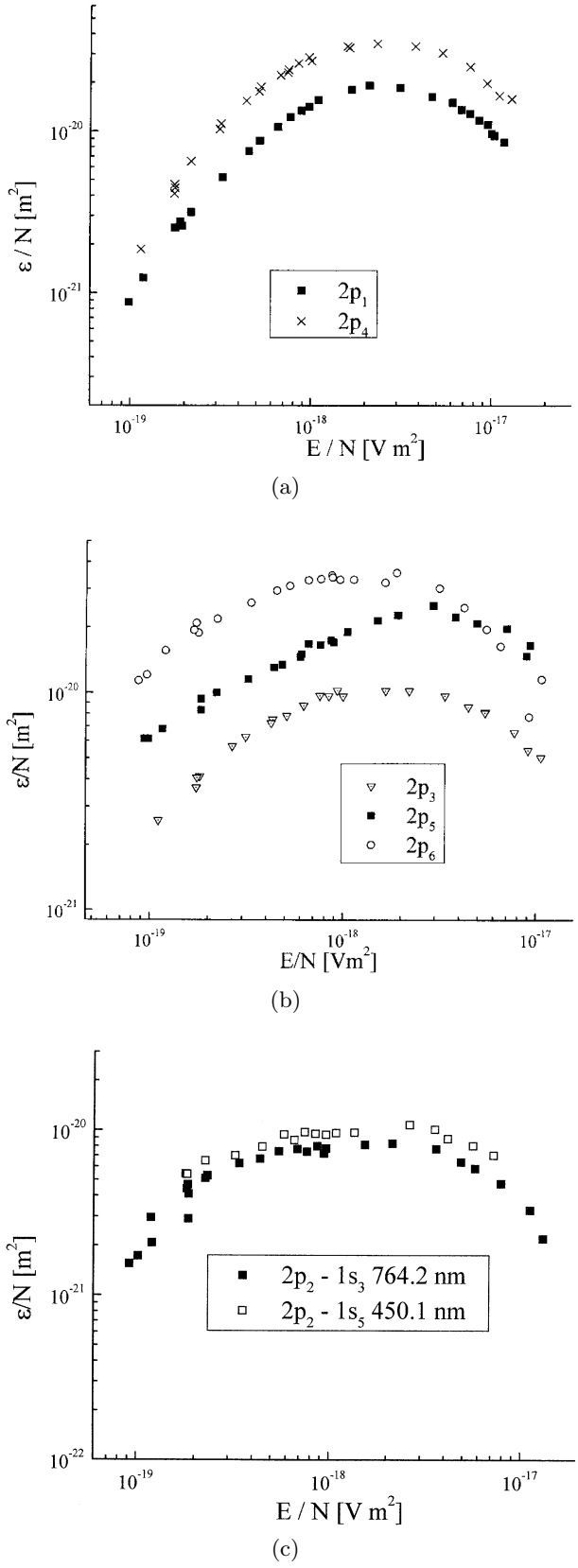

Fig. 3. Excitation coefficients for $2p_1$ and $2p_4$ levels of xenon (a); for $2p_3$, $2p_5$ and $2p_6$ levels of xenon (b); for $2p_2$ levels of xenon based on two transitions (c).

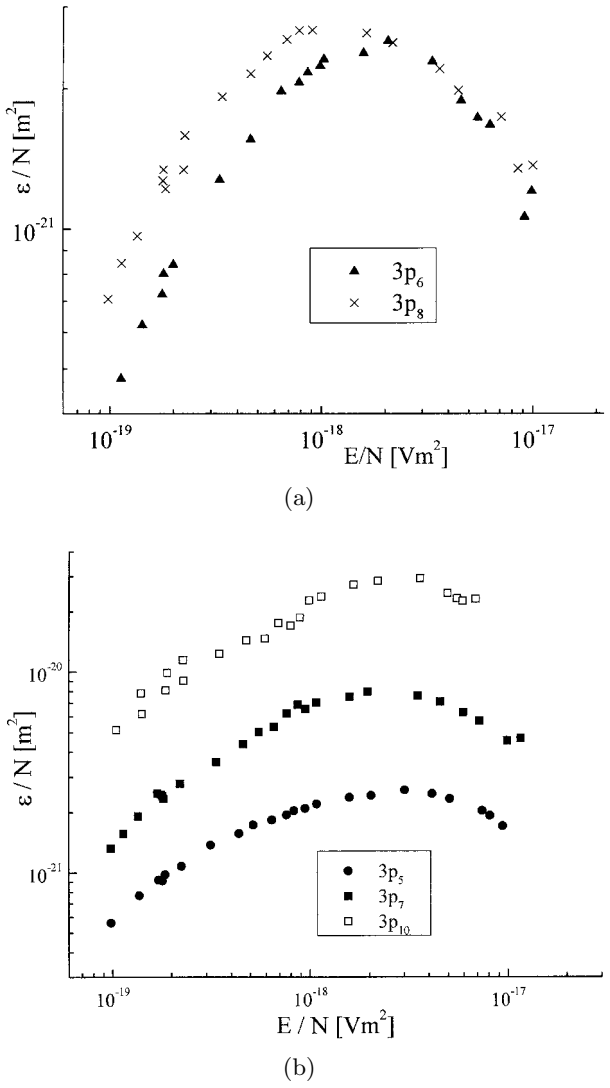

Fig. 4. Excitation coefficients for $3p_6$ and $3p_8$ levels of xenon (a); for $3p_5$, $3p_7$ and $3p_{10}$ levels of xenon (b).

4 Conclusion

In this paper we have presented the data on excitation coefficients for six $2p$ levels ($2p_1$, $2p_2$, $2p_3$, $2p_4$, $2p_5$, $2p_6$) and five $3p$ levels ($3p_5$, $3p_6$, $3p_7$, $3p_8$, $3p_{10}$) of xenon. Excitation coefficients were obtained for a wide range of E/N, from 90×10^{-21} Vm^2 to about 1×10^{-18} Vm^2. The emission data were normalized by absolute calibration of the detection system by using a tungsten ribbon lamp. The spatial distribution of emission was measured as well and normalized to the excitation coefficient at the anode. Many of the $2p$ and $3p$ levels showed extensive collision coupling with nearby levels and consideration of the kinetics of all coupled levels is necessary in order to obtain the cross-sections by the swarm analysis.

Absolute values of the excitation coefficient which is obtained from the emission are not only the result of direct electron induced excitation. Most of the $2p$ and $3p$

levels have strong collisional coupling with the nearby levels. Therefore one need to specify all the coupled channels of population and depopulation in order to compare the present data with the data for direct electron excitation. Cross-sections measurements for different processes in xenon are not sufficiently complete. Unlike the situation for argon and neon the measurements of the cross-sections for excitation of different transitions of xenon are rare and published results differ by order of magnitude. Consequently it is very difficult to make a complete kinetic model but we hope that the present data could be used to improve the situation. On the other hand the present data may be used directly in plasma diagnostics by applying simplified kinetics with the aid of effective excitation coefficients.

It was not possible to find other sources of data for Xe excitation coefficients so we cannot make comparisons. On the other hand most sets of cross-sections have effective, lumped cross-sections so we cannot make comparisons with such calculations either.

The authors acknowledge partial support of 01E03 MNTRS project and contribution of Dr. B. Jelenković in development of some aspects of the experimental system and useful discussions with Dr. A.V. Phelps and Dr. N. Sadeghi.

References

1. R. Shuker, A. Gallagher, A.V. Phelps, J. Appl. Phys. **51**, 1306 (1980).
2. R.J. Morley, J.J. Wendland, H.J. Baker, D.R. Hall, Opt. Commun. **142**, 244 (1997).
3. T.L. Dutt, J. Phys. B **2**, 234 (1969).
4. M.V. Malyshev, V.M. Donnelly, J. Vac. Sci. Technol A **15**, 550 (1997).
5. K. Johannsen, E. Schenuit, H. Spitzer, R. Vick, G. Westerkamp, Nucl. Instr. Meth. A **283**, 702 (1989).
6. A. Bolozdynya, V. Egorov, A. Koutchenkov, G. Safronov, G. Smirnov, S. Medved, V. Morgunov, Nucl. Instr. Meth. A **385**, 225 (1997).
7. J.P. Boeuf, L. Garrigues, L.C. Pitchford, *Electron Kinetics and Applications of Glow Discharges*, edited by U. Kortshagen, L.D. Tsendin, NATO ASI Series B: Physics **367**, 85 (1998).
8. T. Tokonami, T. Makabe, J. Appl. Phys. **72**, 3323 (1992).
9. M.F. Dony, F. Debal, M. Wautelet, J.P. Dauchot, M. Hecq, J. Bretagne, P. Leray, A. Ricard, J. Phys. III France **7**, 1869 (1997).
10. M.F. Dony, A. Richard, J.P. Dauchot, M. Hecq, Surf. Coat. Techn. **74-75**, 479 (1995).
11. V.P. Nagorny, P.J. Drallos, Plasma Sources Sci. Technol. **6**, 212 (1997).
12. C. Punset, J.P. Boeuf, L.C. Pitchford, J. Appl. Phys. **83**, 1884 (1998).
13. Z.M. Jelenak, Z.B. Velikić, J.V. Božin, Z.Lj. Petrović, B.M. Jelenković, Phys. Rev. E **47**, 3566 (1993).
14. Z. Stokić, M.M.F.R. Fraga, J. Božin, V. Stojanović, Z.Lj. Petrović, B.M. Jelenković, Phys. Rev. A **45**, 7463 (1992).
15. V. Stojanović, J.V. Božin, Z.Lj. Petrović, B.M. Jelenković, Phys. Rev. A **42**, 4983 (1990).
16. G.N. Malović, J.V. Božin, B.M. Jelenković, Z.Lj. Petrović, Nucl. Instr. Meth. B **129**, 317 (1997).
17. B.M. Jelenković, A.V. Phelps, Phys. Rev. A **36**, 5310 (1987).
18. Z.Lj. Petrović, A.V. Phelps, Phys. Rev. E **56**, 5920 (1997).
19. M. Aymar, M. Coulombe, At. Data Nucl. Data Tables **21**, 537 (1978).
20. G. Inoue, J.K. Ku, D.W. Setser, J. Chem. Phys. **81**, 5760 (1984).
21. W.J. Alford, J. Chem. Phys. **96**, 4330 (1992).
22. Z.Lj. Petrović, V.D. Stojanović, J. Vac. Sci. Technol A **16**, 329 (1998).
23. A.A. Kruithof, Physica **7**, 519 (1940).
24. L. Jacques, W.B. Bruynooghe, R. Boucique, W. Wieme, J. Phys. D **19**, 1731 (1986).
25. A.K. Bhattacharya, Phys. Rev. A **13**, 1219 (1976).
26. T.J. Sommerer, J. Phys. D: Appl. Phys. **29**, 769 (1996).